Astron. Astrophys. 289, 972–982 (1994)

ASTRONOMY
AND
ASTROPHYSICS

Temporary capture of grains in exterior resonances with the Earth: Planar circular restricted three-body problem with Poynting–Robertson drag

M. Šidlichovský* and D. Nesvorný**

Astronomical Institute, Boční II 1401, 141 31 Praha 4, Czech Republic

Received 29 November 1993 / Accepted 20 April 1994

Abstract. The orbital evolution of the dust grains of radius $\sim$ 10 μm, close to the exterior resonances with the Earth is investigated. Especially resonances 6/7, 5/6 and 4/5 were studied as they are close enough to the Earth orbit and our numerical experiments proved their higher capture efficiency. Numerical simulations were compared to the semi-analytical approach of the circular restricted problem with Poynting-Robertson drag. The disturbing function has been averaged over the fast variable numerically. It was shown that due to convergence problems the disturbing function cannot be approximated by the usual truncated series. Even if the terms of the fourth order in eccentricity e are included, a qualitatively different picture is obtained. Using the semi-analytic approach we found stationary solutions where the resonance effect cancels the drag. Where there is capture in numerical simulations, the solution clearly approaches these stationary points. The amplitude of the resonant variable is, however, slowly increasing which has to lead eventually to close approach to the Earth, and the capture is only temporary. The particle may be trapped even for times of the order of 10^5 years in the circular case.

The equations linearized numerically in the vicinity of stationary point were shown to lead to one real negative frequency and two complex conjugate frequencies with a positive real part for typical values of the parameters. This shows the instability of the stationary point. The β-dependence of the stationary points positions is given. For $\beta \sim 0.1$ and larger, these stationary points are much too close to the collision curve, where the averaging method fails and the particle will soon be removed by close approach to the Earth. Some inferences for the possible distribution of grains in the vicinity of the Earth orbit are made. The effect of other planets has been shortly discussed. It was shown that temporary trapping is still possible, only the time of capture is shorter.

Key words: interplanetary medium – celestial mechanics

Send offprint requests to: M. Šidlichovský

* e-mail address: SIDLI at SEIS.IG.CAS.CZ

** *Present address:* University of São Paulo, Brazil

1. Introduction

The radiation force $\boldsymbol{F}$ acting on a particle of unit mass is

$$\boldsymbol{F} = \beta G \frac{m_{\odot}}{r^2}\left[(1-\frac{\dot{r}}{c})\frac{\boldsymbol{r}}{r} - \frac{\boldsymbol{v}}{c}\right] \tag{1}$$

and it consists of radiation pressure and the velocity dependent part, the so-called Poynting-Robertson (PR) drag. Here G is the gravitational constant, $\boldsymbol{r}$ is the orbital radius vector of the grain particle, $\boldsymbol{v}$ its velocity, $m_{\odot}$ is the mass of the Sun, and c is the speed of light. The PR drag and the value of parameter β are discussed in detail by Burns et al. (1979). It was shown that β is related to the radiation pressure coefficient $Q_{\rm pr}$ as

$$\beta = 5.7\, 10^{-5}\frac{Q_{\rm pr}}{\rho s}, \tag{2}$$

where radius s and density ρ of the particle are in cgs units. Having employed the Mie theory to determine $Q_{\rm pr}$, Burns et al. (1979) presented the dependence of β on radius s for various materials. Most of our numerical simulations were performed with $\beta = 0.01$, corresponding to radius $s \sim 20\,\mu$m (for $\rho \sim 3$ g/cm^3 and geometrical optics limit $Q_{\rm pr} = 1$). The semi-analytical calculations, especially the determination of stationary points, were performed for various β.

It is well-known that the orbit of a dust particle around the Sun under gravitational and radiation forces, Eq. (1), evolves so that both its semimajor axis a and its eccentricity e decrease. The problem is integrable and the time evolution of e and a can be expressed in quadratures (Wyat et al. 1950). The possibility of resonant capture of the falling particle in the interior resonance 2/1 was studied by Gonzi et al. (1982). They concluded that the grains always cross the resonance region without any oscillation.

For the exterior resonances the possibility of resonant capture was first documented in numerical simulations by Jackson & Zook (1992). They showed that a 100-μm-radius grain, released at perihelion passage from asteroid Hungaria, would be captured at the 5/6 resonance with the Earth for more than 10^5 y.

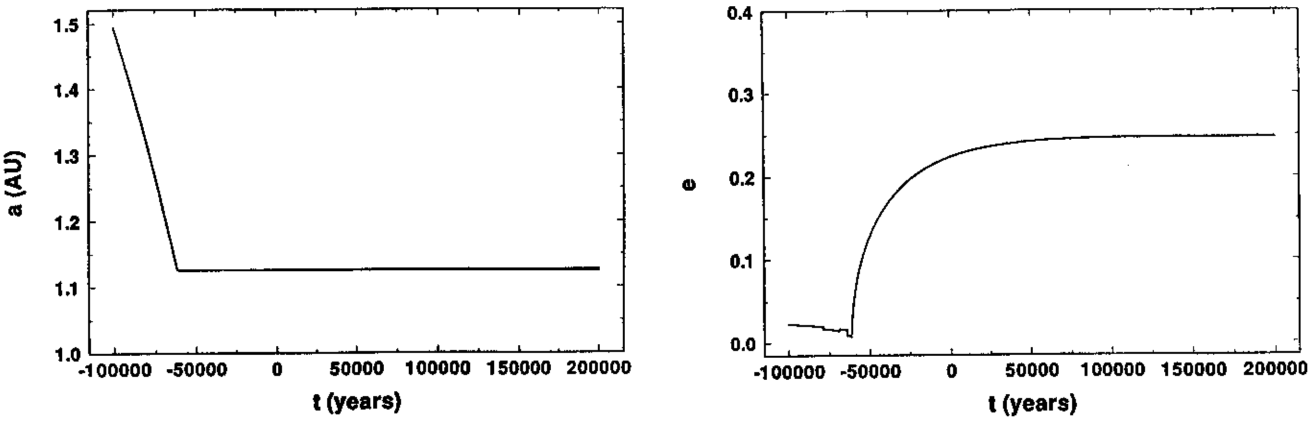

Fig. 1. The particle is captured in the 5/6 resonance

The slow decrease of the semimajor axis is stopped, and eccentricity sharply increases to some limiting value. These results stimulated our investigations.

The different behaviour while passing through the exterior and interior resonances was explained by Weidenschilling & Davis (1985) in their study of planetesimal orbit in resisting gas medium and by Sicardy et al. (1993) for the grain particle with PR drag. They showed that, while for exterior resonances the resonant contribution may compensate the radiation decrease of the semimajor axis and stationary points may exist, this is impossible for the interior resonances. The interior resonances in the restricted three-body problem were studied in many papers in relation to the existence of the asteroid belt and its resonant structure (Kirkwood gaps). The possibility of the capture of the grains in exterior resonances made it necessary to study first these resonances in the simplest planar restricted problem without PR drag to understand the phase space of the problem, its singular solution, etc. This gap was filled by Beaugé (1993) who proved the existence of asymmetric libration centres (ALC) for the 1/2 and 1/3 exterior resonances using the averaging of disturbing function. The ALC were first found by Message (1958) who used a truncated disturbing function. They do not appear at interior resonances. We found no ALC at exterior resonances 6/7, 5/6 and 4/5, even if they seem to be there (e.g. for 5/6) if one employs a truncated disturbing function of the fourth degree in eccentricity. This difference indicates that the truncation method is unsuitable for these resonances. Indeed, the Sundman (1915) condition for convergence of the series for the disturbing function clearly shows that the series is divergent for a corresponding to these resonances at e corresponding to the ALC obtained by the truncation method, see the discussion in Sect. 4. To determine the stationary points we used the quite general equations of Beaugé & Ferraz-Mello (1993a). Our Eqs. (18) are expressed in different variables but they may be shown to be equivalent to Beaugé & Ferraz-Mello (1993b, Eq. (14)). They applied this approach to the 1/2, 2/3 and 1/3 resonances Beaugé & Ferraz-Mello (1993b). They used the adiabatic invariant theory and discussed the capture probability of the particle in these resonances. For each resonance they found an eccentricity limit under which the capture probability is 100%. These results cannot be applied to the Earth's resonances 1/2, 1/3 and 2/3 as the condition of adiabacity is not fulfilled there because μ for the Earth is too small (Beaugé and Ferraz-Mello used value close to Jupiter's). Our numerical experiments show that the capture is more probable at the higher first-order resonances. These resonances were not investigated in Beaug & Ferraz-Mello papers as for their high value of μ these resonances overlap and capture is not observed there.

2. Numerical simulations for the simple planar and circular model

2.1. The capture

When a dust particle approaches some exterior resonance the orbit begins to exhibit characteristic changes. The gradual decay of the semimajor axis due to the dissipative force is being broken the eccentricity suddenly jumping at the same time. It is known from the Jackson & Zook (1992) study that, under some circumstances, this can lead to the long-term capture. We decided at first to investigate this capture numerically in order to obtain basic knowledge of the orbit's evolution, hoping to find even partial answers to these questions. What resonance can serve as a trap and what are the initial conditions which lead to the trapping? What is the role of the β-parameter and the perturber mass?

Let us assume one planet in a circular orbit with radius a_1, and watch a dust particle released at $a > a_1$. It is influenced by the Sun and the planet's gravitational force and by radiation forces, Eq. (1). For the complete differential equation refer to the next section, Eq. (3).

We performed many numerical integrations of this problem with different initial conditions using the programming package written originally for integrating the $N+M$ body system by one of us (D.N.) in C-language. It is the system, where N primary bodies are interacting (the Sun and planets) and M secondary bodies (asteroids, dust particles) are influenced by them. The secondary bodies neither interact among themselves, nor do they influence the primary bodies. In application to our simple

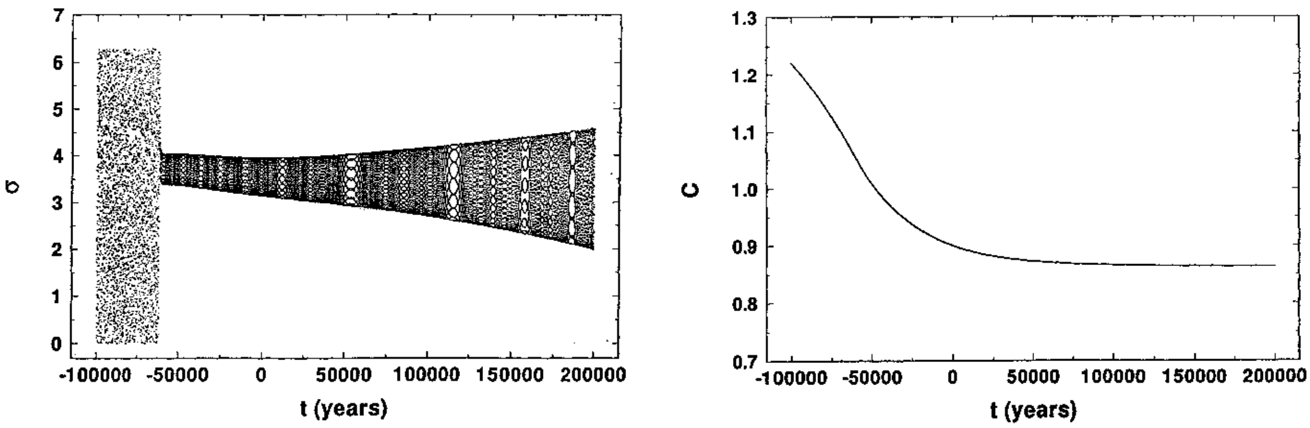

Fig. 2. Resonant parameter and averaged Jacobi constant in the time dependence

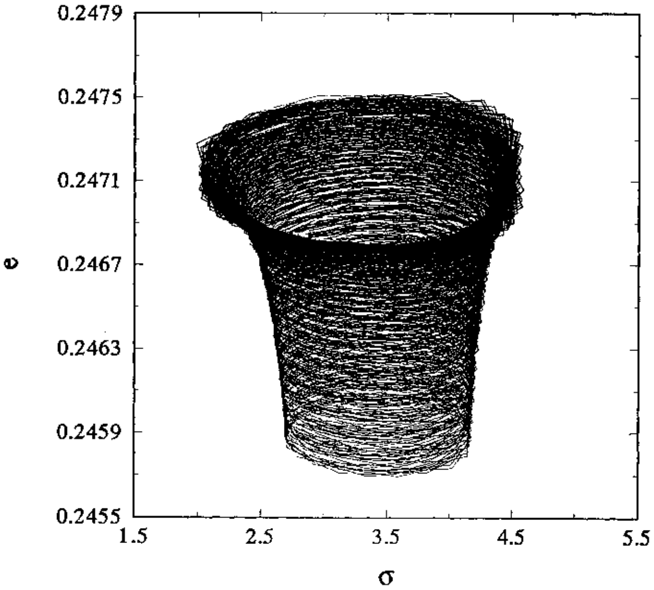

Fig. 3. Eccentricity-resonant variable evolution

model only two primary bodies are included, and the radiation forces are switched on. Various numerical methods may be used, but we employed the symmetric multistep method of the twelfth order (Quinlan & Tremaine 1990) which is specially convenient for near-Keplerian system investigations.

Figure 1 shows the typical situation of a capture at the $5/6$ resonance with the Earth for the $\beta = 0.01$ particle. The decay of the semimajor axis was stopped at $a \sim 1.125$ AU. At the same time the eccentricity begins to increase. This causes the particle to cross the Earth's orbit starting at $e \sim 0.112$ but keeping the same evolution further on. Obviously, there is some protecting mechanisms which prevents a close approach during the later evolution. We will come to an explanation later on. During the next period the eccentricity increases approaching the value ~ 0.2472. There are oscillations hardly visible on the scale chosen for the figures. Their range slowly increases for both a and e to values ~ 0.003 AU and ~ 0.0007, respectively at $t = 2.\,10^5$ y. This capture is found to be temporary, because just after $t = 2.\,10^5$ y, the particle reaches the distance of ~ 0.007 AU from the Earth which causes its removal.

We can now compute the resonant variable σ usually used (see the definition later, Eq. (6)) and the averaged Jacobi constant C (Eq. 12). Figure 2 shows their evolution for the same initial conditions which were used earlier. As expected, σ begins to librate when the particle is trapped in the resonance. The increase in amplitude leads to the libration range of $\sim 150°$ at the end of integration. The original decrease of C slows down as its value approaches ~ 0.8635 .

Another interesting plot can be obtained by combining the time evolution in e and σ (Fig. 3). Here the position spirals from the bottom to the top due to the long-term change in eccentricity, but this vertical evolution is very slow. One can describe this behaviour as librations around a slowly varying centre. The period of these librations is about 200 y, the slowly changing amplitudes in σ and e can be estimated from this figure as well.

This capture case was chosen to present the typical orbit evolution. A wide spectrum of initial conditions leads to the trapping at $5/6$, but many of them exhibit large oscillation in σ at the beginning, and they are removed in a shorter time, usually of the order of 10^4 y. There is a clear relation between the σ-oscillation range at the begining and the capture time.

2.2. *Statistics*

Let us now go back to our original questions concerning the capture possibility in various resonances. From the practical point of view we can investigate two kinds of planetary bodies. Some like Jupiter with $m \sim 10^{-3}\, M_\odot$ or Earth-like bodies with $m \sim 2.5\, 10^{-6}\, M_\odot$. The main part of this work is devoted to the exterior resonances with the Earth, although several comments on a more massive perturber are made.

In investigating the $(p+q)/p$ resonance (for the exterior resonance p is negative) we chose $\beta = 0.01$ and introduced initial conditions $a = a_{res} + 0.005$ AU and $e = 0$. We then spreads 36 particles along the whole circle at equidistant angular distances of 10 degrees. For the first-order resonances ($q = 1$) and

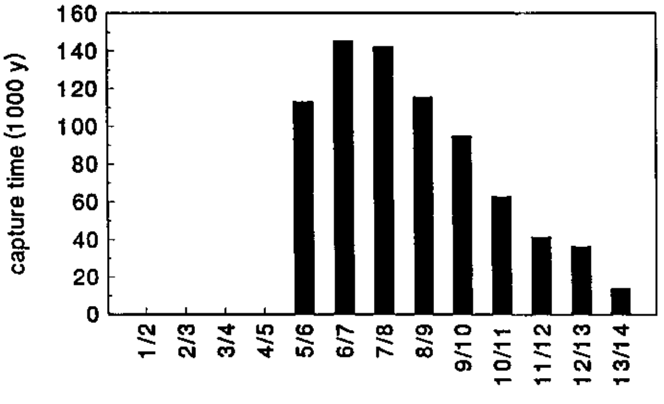

Fig. 4. Capture times for different first-order resonances and $\beta = 0.01$

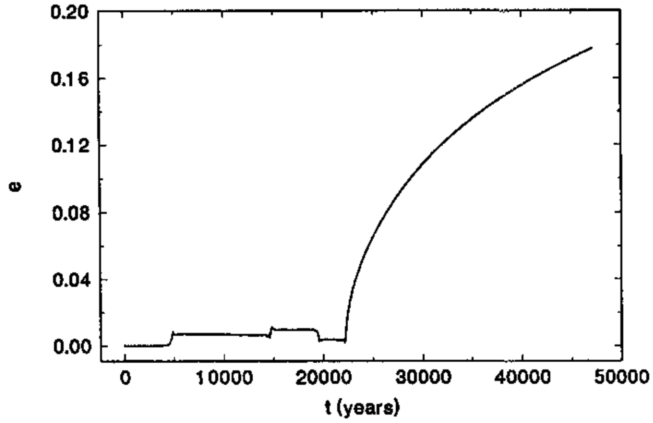

Fig. 5. The particle is captured in 5/6 after passing 2/3, 3/4 and 4/5

$-14 \leq p \leq -2$ this set of initial conditions was integrated sufficiently long to see if capture occurred. The result is unequivocal; for $p \geq -5$ no trapping was detected, and starting at $p = -6$ all particles were captured. To verify this, almost a hundred particles initially spread along the circle were integrated, but no capture was observed for 4/5.

Even higher degree resonances $p < -14$ can catch particles (the degree of the resonance is defined here as $|p|$). But it was observed that the capture is much shorter due to resonance overlapping and the ~ 0.001 AU oscillations at the beginning. The same effect is more important for more massive bodies. We did not succeed in finding long-term capture at the 5/6 with Jupiter. Although we were concentrating on the first-order resonances, we found several cases when the second-order resonance served as a trap (for instance 9/11).

Figure 4 describes another of our approaches. We prolonged the integration up to 200 000 y trying to estimate the capture time for various resonances. The particles probably having the shortest capture time (with the largest oscillations at the beginning) were picked up from our set. We could thus estimate the bottom limit. For the 5/6 resonance and our set of initial conditions the particles were observed to have a life time longer than 100 000 y and up to 140 000 y in agreement with our assumption.

The step between 4/5 and 5/6 crosses the boundary between the passage through and the capture for $\beta = 0.01$. If we increase β to 0.02 then this boundary shifts and no capture in 5/6 occurs. We succeeded in locating the boundary between 7/8 and 8/9. For $\beta = 0.04$ it appears between 8/9 and 9/10. On the other hand, if we decrease β to 0.001 then even the 2/3 resonance has the trapping capability, and the boundary shifts between 1/2 and 2/3. In this case it was found that the capture times extended to more than 200 000 y. To summarize one can say that if β is increased the low degree resonances become uneffective. For each value of β there exists one resonance (the lowest of the effective resonances) which should capture the majority of particles. We wondered how the non-zero eccentricity can influence the capture probability. At first we examined the effect of the low-order resonances which cause the eccentricity jumps during particle passage. Again we chose 36 particles $\beta = 0.01$ with an initially circular orbit $a = 1.35$ AU outside 2/3. Every particle of this set should first cross several uneffective resonances (2/3, 3/4, etc.) and meet both 4/5 and 5/6 with non-zero eccentricity. Figure 5 describes the typical eccentricity evolution. The jumps approximately at 5000 y, 14500 y and 19000 y refer to the 2/3, 3/4 and 4/5 resonances. The particle is then captured at 5/6. But this appeared only in 10 cases. Contrary to our previous idea, 15 particles were captured in 4/5, i. e. before reaching the previously found boundary. The rest of the 11 particles passed even 5/6 and was trapped partially in 6/7 and 7/8. It makes the result of our initial statistics more smeary, but preserves the general idea of the capture probability's dependence on β.

We did not try to extend these statistics to the initially elliptic orbits because it gives the problem more degrees of freedom, and this needs much more computer time. On the other hand, with the knowledge which we gained from the analytical study we succeeded in finding suitable initial conditions for $\beta = 0.01$ and even for the 2/1 resonance capture, but they are very rare in phase space, and it is no wonder that no particle from our set was captured there.

3. Basic equations

Let us investigate the simple planar and circular model introduced in Sect. 2. The heliocentric radius vector of the dust particle is $\boldsymbol{r}$. Corresponding variables for the planet (the Earth) will be distinguished by the subscript 1, so that $\boldsymbol{r}_1$ is the heliocentric radius vector of the planet. As usually a is the semimajor axis, e the eccentricity, λ the mean longitude, $\tilde{\omega}$ the longitude of the pericentre. The equation of motion for the dust particle perturbed by the radiation force and gravitational attraction of the planet of mass m_1 is

$$\ddot{\boldsymbol{r}} = \nabla \mathrm{G}\frac{m_{\odot}(1-\beta)}{r} + \nabla R + \boldsymbol{Y}\,, \tag{3}$$

where the disturbing function

$$R = \mathrm{G}m_1\left(\frac{1}{|\boldsymbol{r}-\boldsymbol{r}_1|} - \frac{\boldsymbol{r}_1\boldsymbol{r}}{r_1^3}\right) \tag{4}$$

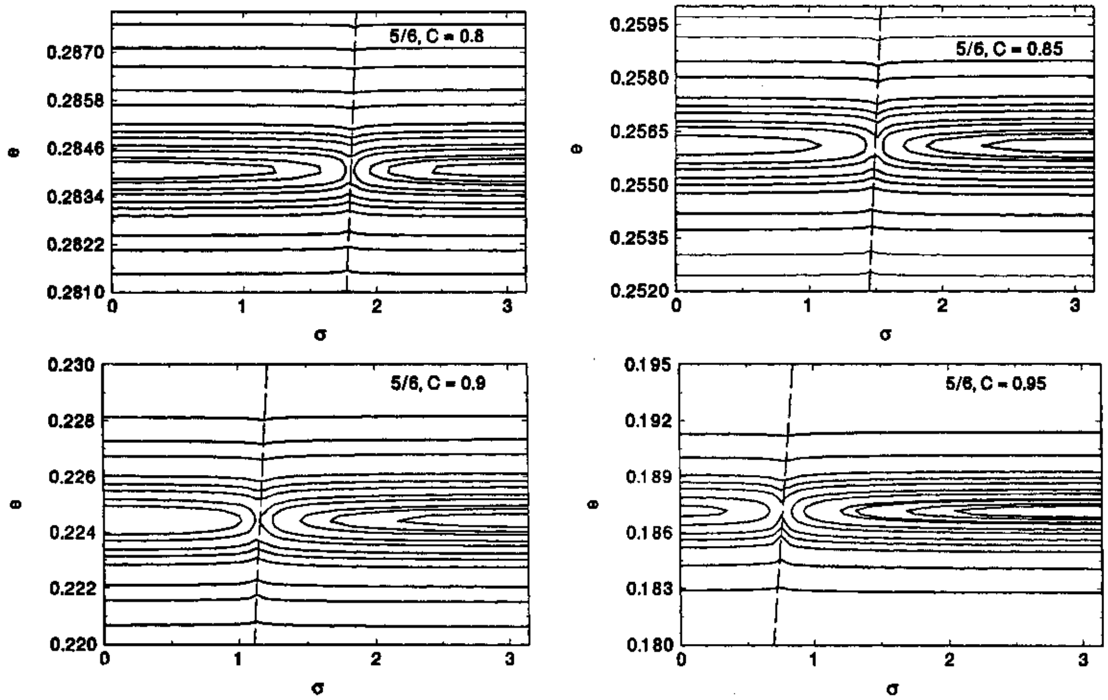

Fig. 6. The level curves of constant H for four different values $C = 0.8, 0.85, 0.9, 0.95$ for the 5/6 resonance

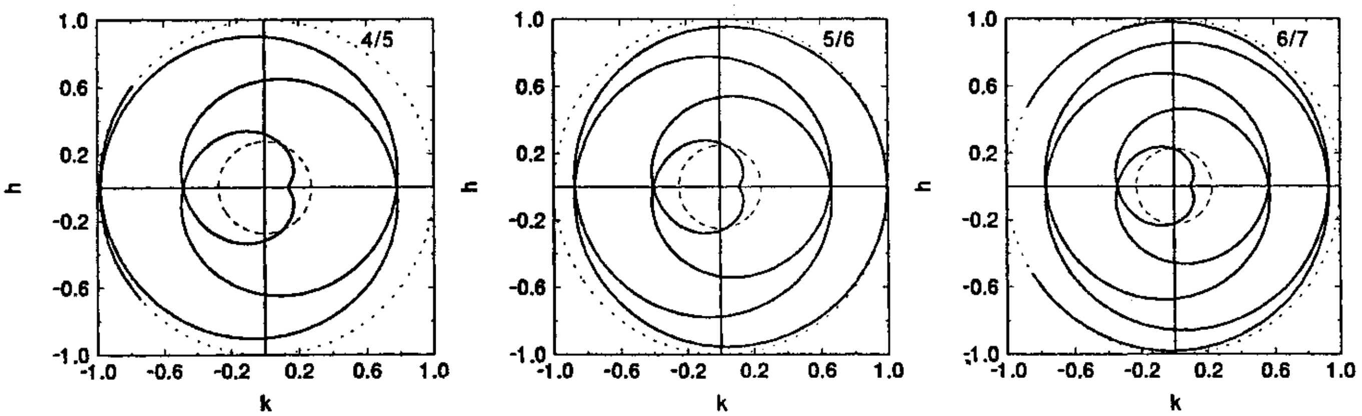

Fig. 7. The collision curves which form the set of points where disturbing function R has a singularity due to the collision of the grain particle with the Earth

and the PR drag $\boldsymbol{Y}$ follows from (1),

$$\boldsymbol{Y} = -\beta \mathrm{G}\frac{m_\odot}{r^2}\left(\frac{\dot{r}\boldsymbol{r}}{cr} + \frac{\boldsymbol{v}}{c}\right). \tag{5}$$

Strictly speaking Eq. (3) is valid only for $m_1 = 0$ but as the correction to term $\boldsymbol{Y}$ is of order $\sim m_1\boldsymbol{Y}$, it may be neglected. As we assume that the system is close to resonance, we shall introduce the canonical variables $\sigma, J, \sigma_1, J_1, \sigma_2, J_2$ used to study resonances in the asteroid belt for the planar three-body problem (Ferraz-Mello et al. 1993)

$$\begin{aligned} q\sigma &= (p+q)\lambda_1 - p\lambda - q\tilde{\omega}, \\ q\sigma_1 &= (p+q)\lambda_1 - p\lambda - q\tilde{\omega}_1, \\ q\sigma_2 &= \lambda - \lambda_1, \end{aligned}$$

$$\begin{aligned} J &= L - G, \\ J_1 &= G + \frac{\Lambda}{n_1}, \\ J_2 &= (p+q)L + \frac{p}{n_1}\Lambda. \end{aligned} \tag{6}$$

In Eq. (6) n_1 is the mean motion of the planet, Λ is the canonical variable conjugated to time, L, G are the Delaunay variables connected to eccentricity e and semimajor axis of the particle a

$$\begin{aligned} L &= (\kappa a)^{1/2}, \\ G &= L\left[1 - \left(1 - e^2\right)^{1/2}\right], \\ \kappa &= \mathrm{G}m_\odot(1-\beta). \end{aligned} \tag{7}$$

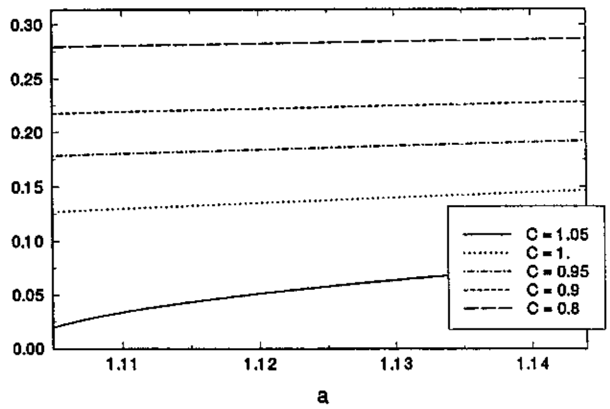

Fig. 8. Dependence of e on a for various fixed C

Following the method employed by Beaugé & Ferraz-Mello (1993a) and Beaugé (1993), after averaging over fast variable σ_2 we obtain a system similar to the Hamilton canonical equations with additional drag terms,

$$\begin{aligned} \dot{\sigma} &= \frac{\partial H}{\partial J}, \\ \dot{\sigma}_1 &= \frac{\partial H}{\partial J_1}, \\ \dot{\sigma}_2 &= \frac{\partial H}{\partial J_2}, \\ \dot{J} &= -\frac{\partial H}{\partial \sigma} - \langle P_2 \rangle, \\ \dot{J}_1 &= -\frac{\partial H}{\partial \sigma_1} + \langle P_1 + P_2 \rangle, \\ \dot{J}_2 &= (p+q)\langle P_1 \rangle, \end{aligned} \tag{8}$$

with the Hamiltonian

$$H = \frac{\kappa^2}{2}\left[\frac{J_2}{q} - \frac{p}{q}(J + J_1)\right]^{-2} + \Lambda - \langle R \rangle, \tag{9}$$

where

$$\langle R \rangle = \frac{1}{2\pi}\int_0^{2\pi} R \mathrm{d}\sigma_2 \tag{10}$$

and

$$\begin{aligned} \langle P_1 \rangle &= -Qn\gamma^{-3}\left(1 + \frac{3}{2}e^2\right), \\ \langle P_2 \rangle &= Qn\gamma^{-3}\left(1 + \frac{3}{2}e^2 - \gamma^3\right), \\ Q &= \frac{\mathrm{G}m_\odot \beta}{c}, \quad \gamma = \left(1 - e^2\right)^{1/2}. \end{aligned} \tag{11}$$

Equations (8)-(11) are the basic equations governing our problem. For the circular problem Hamiltonian H is independent of σ_1 and $\frac{\partial H}{\partial \sigma_1} = 0$.

4. Exterior resonances without drag

4.1. The averaging

The investigation of the exterior resonances and their phase space topology received little attention. Recently this question was addressed by Beaugé (1993) who investigated the 1/2, 1/3, 2/3 and 3/4 resonances. In Sect. 2 we saw that resonances 5/6 and 6/7 seem to be more important for the capture of grains into commensurabilities with the Earth. That is why we concentrated on these resonances. The calculations were performed for m_1 equal to the Earth's mass. We used the system of units where $\mathrm{G} = 1$, $a_1 = 1$ and $m_\odot = 1$.

The problem is described by Eq. (8) with $\beta = 0$ and therefore $\langle P_1 \rangle = \langle P_2 \rangle = 0$. In addition to H we have two other integrals of motion J_1 and J_2. The system is reduced to one degree of freedom. The motion in phase space is described by the level curves of the Hamiltonian. As $\langle R \rangle$ cannot depend on Λ, it depends only on the combination of J_1 and J_2 independent of Λ:

$$\begin{aligned} C &= \kappa^{-1/2}\left(\frac{1}{q}J_2 - \frac{p}{q}J_1\right) \\ &= a^{1/2}\left[1 + \frac{p}{q} - \frac{p}{q}\left(1 - e^2\right)^{1/2}\right]. \end{aligned} \tag{12}$$

We shall denote

$$\langle R \rangle = \mathscr{R}(C, e, \sigma). \tag{13}$$

For a given C averaging in Eq. (10) is easily performed by a simple program using Eq. (4) and the well-known relation between the rectangular coordinates and the canonical coordinates defined in Eq. (6). Figure 6 shows the interesting part of phase space of resonance 5/6 for four different values of C. With increasing C the resonance region is shifted to smaller values of e. The dashed curve is the collision curve where $\mathscr{R}$ has a singularity corresponding to the collision of the particle with the Earth (Ferraz-Mello et al. 1993). The collision curves for the 4/5, 5/6 and 6/7 resonances are shown in Fig. 7. Here

$$k = e\cos\sigma, \quad h = e\sin\sigma. \tag{14}$$

For a given resonance (p, q) and given C, only a small strip of e is relevant. For the 5/6 resonance, for instance, a should be restricted to interval $a \in (1.119, 1.145)$, otherwise the system will be closer either to the 4/5 or the 6/7 resonance. The dependence of e on a for different values of C Eq. (12) is given in Fig. 8, where the boundaries of a correspond roughly to the required interval. The range of possible e is restricted to a very small interval which may be estimated from Fig. 8 for a given C. That is why it is much more reasonable to illustrate the phase space for only a small interval in e.

For the 4/5 and 6/7 resonance we get very similar patterns, Fig. 9. The special choice of C will be obvious from the results of Sect. 5 (this C is close to C_0 corresponding to the stationary point). In the vicinity of the collision curve the formulation with the averaged Hamiltonian is bound to fail as for close approaches

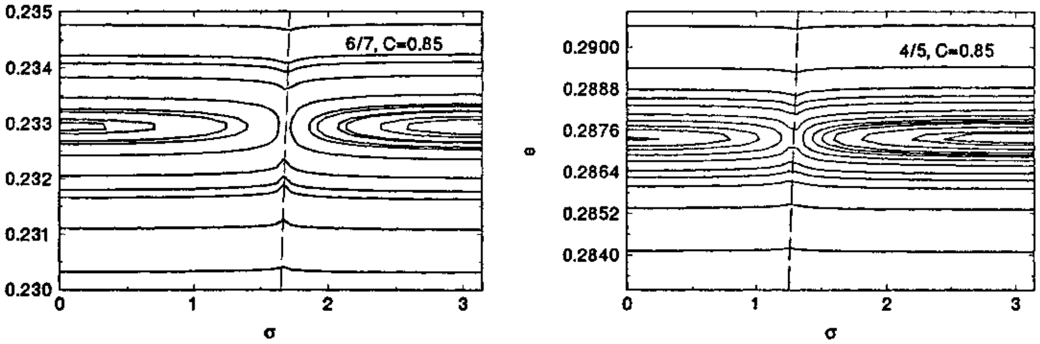

Fig. 9. The typical level curves for the 4/5 and 5/6 resonance, both curves were calculated for $C = 0.85$

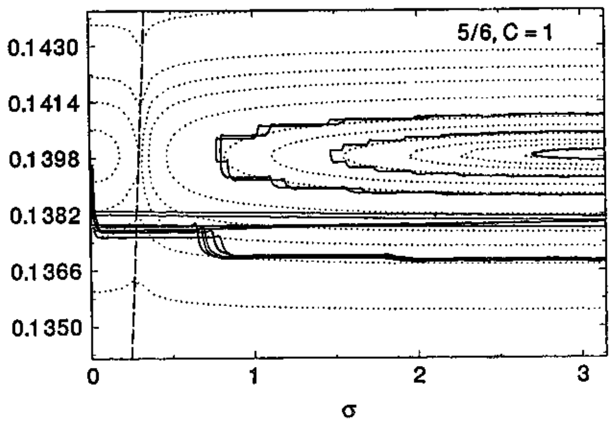

Fig. 10. Comparison of four numerically calculated trajectories with the level curves for the 5/6 resonance (the level curve does not fit the trajectory close to the collision curve well)

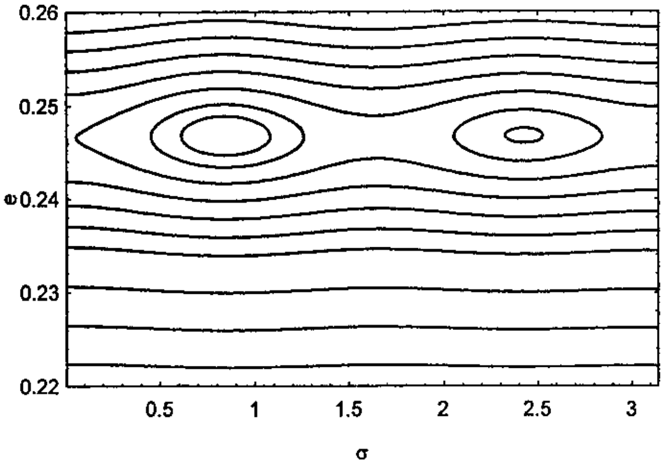

Fig. 11. Level curves calculated for the 5/6 resonance and $C = 0.9$ with the Laplacian expansion truncated at the fourth degree in e

of the particle to the Earth the approximation of the Earth mass by the smeared ring must be inadequate. To illustrate the region of applicability of the averaging approach we compared four trajectories calculated numerically with the level curves of the Hamiltonian, Fig. 10. For most of the time the particle is far from the Earth and e is nearly constant. During conjunctions there are abrupt changes in the eccentricity. In spite of these kicks at conjunctions three curves fit the level of curves quite well, only the effect of the Earth is smoothed over a longer time period. The fourth trajectory copies the level curves only if they are far from the collision curve. When it is brought with them to the vicinity of the collision curve it can cross it freely, and its behaviour differs from the guiding level curves. Figure 10 gives a hint of how far from the collision curve is far enough in the case of the Earth.

4.2. The truncated Laplacian expansion of the disturbing function

We tried to use the Laplacian expansion for the disturbing function by taking into account terms up to the fourth degree in e. Coefficients in this expansion were calculated using the method and program described by Šidlichovský (1991). For resonance 1/2 Beaugé (1993) used only the second-degree approximation and found good agreement with the numerical averaging method.

Figure 11 shows the level curves calculated by the truncation method for the 5/6 resonance and $C = 0.9$. We can see important differences between Fig. 11 and Fig. 6. We did not find any ALC with the averaging method but they are present in Fig. 11. These differences must be caused by poor approximation of the disturbing function with only the beginning of the series. In fact it may be shown that the Laplacian series is absolutely divergent in the region of interest. The Sundman (1916) criterion for the absolute convergence of the Laplacian expansion for $a > a_1$ is

$$a_1 F(e_1) < a f(e), \tag{15}$$

where

$$\begin{aligned} F(g) &= \sqrt{(1+g^2)}\cosh w + g + \sinh w \\ f(g) &= \sqrt{(1+g^2)}\cosh w - g - \sinh w \end{aligned} \tag{16}$$

and

$$w = g \cosh w, \tag{17}$$

see discussion by Ferraz-Mello (1993). Figure 12 shows the boundary between the convergence and divergence region calculated from the Sundman criterion with $a_1 = 1$ and $e_1 = 0$. For

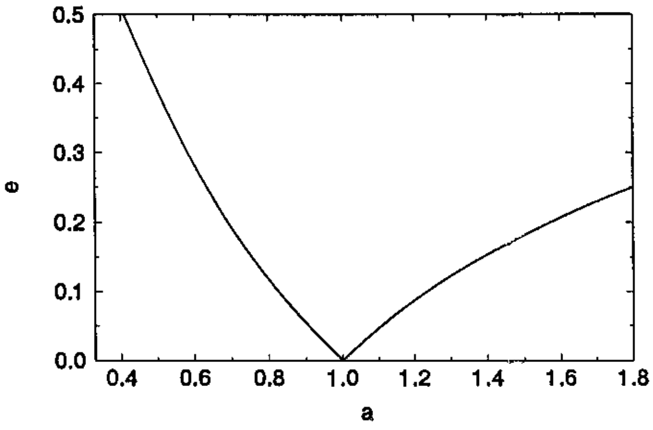

Fig. 12. The boundary curve between the convergence and divergence regions for the Laplacian expansion of the disturbing function for the circular problem

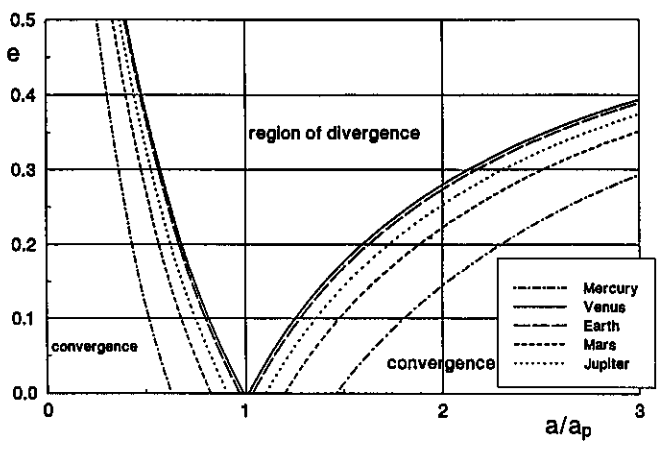

Fig. 13. Boundary between convergence and divergence region for the Laplacian expansion of the disturbing function for some of the planets

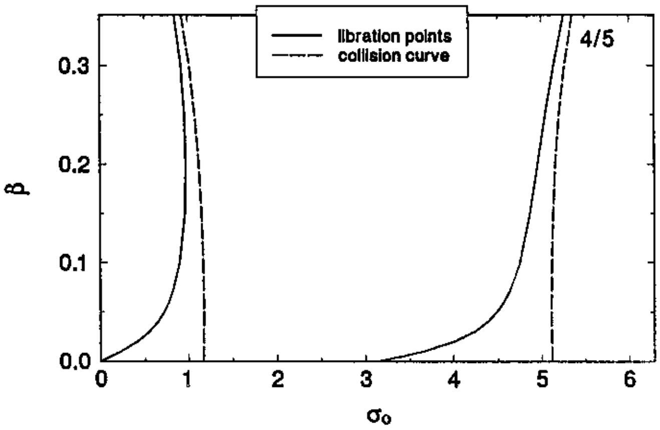

Fig. 14. The dependence of the resonant argument σ_0 on β for the 4/5 resonance

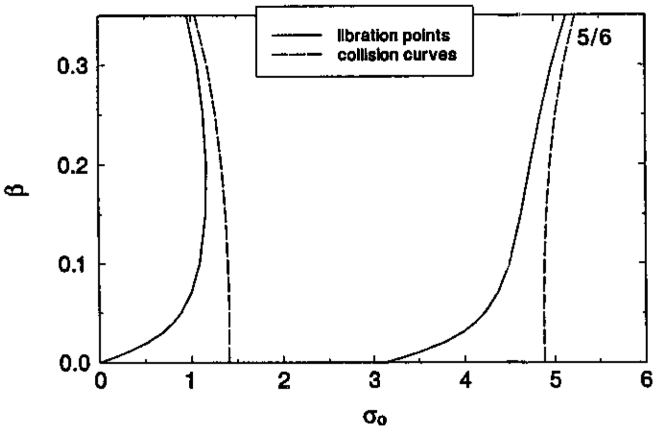

Fig. 15. The dependence of the resonant argument σ_0 on β for the 5/6 resonance

the 5/6 resonance where $a > 1.12$ divergence occurs already for $e = 0.05$ so that the ALC in Fig. 11 are clearly in the region of divergence and the unsuitability of the averaging method is clear. While discussing the convergence of the Laplacian expansion it should be remembered that for the elliptical problem the convergence is even worse. Fig 13 shows the boundaries between the convergence and divergence regions for various planets of the solar system. The differences are caused by their different eccentricities.

5. Libration points in the problem with drag

Libration points for the 1/2, 2/3 and 1/3 commensurabilities were studied by Beaugé & Ferraz-Mello. As resonances 4/5, 5/6 and 6/7 seem to be more efficient for the Earth we will study the libration points for these resonances in the planar circular problem. For each C, σ, e we can determine the averaged disturbing function $\mathscr{R}(C, e, \sigma)$ and its partial derivatives numerically. Libration points are points where C, e, σ are constant. Equations (8) yield get

$$\begin{aligned}
\dot{C} &= \kappa^{-1/2}\left(\langle P_1\rangle - \frac{p}{q}\langle P_2\rangle\right), \\
\dot{e} &= \frac{\gamma}{eL}\left[\left[1+\frac{p}{q}(1-\gamma)\right]\left(\frac{\partial\mathscr{R}}{\partial\sigma}\right) - \langle P_2\rangle - (1-\gamma)\langle P_1\rangle\right], \\
\dot{\sigma} &= \left(1+\frac{p}{q}\right) - n\frac{p}{q} - \frac{\gamma}{eL}\left(1+\frac{p}{q}\frac{e^2}{1+\gamma}\right)\left(\frac{\partial\mathscr{R}}{\partial e}\right).
\end{aligned} \tag{18}$$

If the r.h.s. of Eq. (18) are zero, we have three equations in three variables C, e, σ. These equations may be shown to be equivalent to Eq. (14) in Beaugé & Ferraz-Mello (1993b). The first equation

$$\langle P_1\rangle = \frac{p}{q}\langle P_2\rangle \tag{19}$$

determines the "universal eccentricity" e_0 (see Beaugé & Ferraz-Mello 1993b). The value of e_0 is independent of β and for the resonances in Fig. 4 it is given in Table 1. It is the eccentricity of exact resonance, where a and σ are constant. Our numerical experiments showed that whenever the particle is captured (its

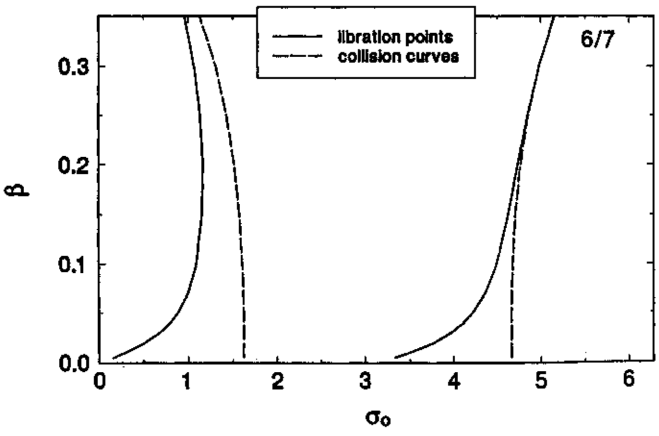

Fig. 16. The dependence of the resonant argument σ_0 on β for the 6/7 resonance

Table 1. The universal eccentricity e_0, resonant semimajor axes a_β and corresponding perihelion and aphelion distances q, Q. The last three columns were calculated for $\beta = 0.01$

$(p+q)/q$	e_0	a_β	q	Q
4/5	0.273610	1.1565	0.8401	1.4730
5/6	0.247226	1.1255	0.8472	1.4037
6/7	0.227254	1.1045	0.8535	1.3555
7/8	0.211455	1.0894	0.8591	1.3198
8/9	0.198552	1.0781	0.8640	1.2921
9/10	0.187756	1.0692	0.8684	1.2699
10/11	0.178549	1.0620	0.8724	1.2517
11/12	0.170577	1.0562	0.8760	1.2363
12/13	0.163585	1.0513	0.8793	1.2233
13/14	0.157389	1.0471	0.8823	1.2119

a is no more decreasing) its eccentricity starts to increase to the value e_0. Employing Eq. (19) we can write the remaining two equations for the libration points in the form

$$\frac{\partial \mathscr{R}}{\partial \sigma} = \langle P_2 \rangle = \frac{Qn}{\gamma^3}\left(1 + \frac{2}{3}e^2 - \gamma^3\right) \tag{20}$$

and

$$\left(1 + \frac{p}{q}\right) - n\frac{p}{q} - \frac{\gamma}{eL}\left(1 + \frac{p}{q}\frac{e^2}{1+\gamma}\right)\left(\frac{\partial \mathscr{R}}{\partial e}\right) = 0. \tag{21}$$

We propose to solve these two equations iteratively. First we put $n = (q+p)/p$ which is the solution of Eq. (21) for $\mathscr{R} = 0$. With this n and $e = e_0$ we can determine C from Eq.(12). We evaluate the r.h.s. of Eq. (20) and determine σ using the program for calculating $\mathscr{R}$ and its partial derivatives. Then we improve the value of n using Eq. (21) with σ obtained in the previous step. We could continue by improving σ from Eq. (20), but this was not necessary as the last correction to a was already of the order of 10^{-4} or smaller. The procedure converges very fast to the libration point e_0, C_0 and σ_0.

Using this iterative procedure we calculated the dependence of σ_0 on β for the 4/5, 5/6 and 6/7 resonances, shown in Figs. 14-16. These figures clearly show that for β close to 0.1 and larger the libration point is too close to the collision curve, and the experience from Fig. 10 indicates that one cannot expect capture in the vicinity of this libration point.

Let us go back to Figs. 1–3. We can now explain many of their features. For $\beta = 0.01$ and the 5/6 resonance we have libration point $e_0 = 0.2472$, $C_0 = 0.8633$, $\sigma_0 = 3.5039$ with corresponding $a_0 = 1.1255$. Values a, e and C in Figs. 1–2 certainly approach these values. Resonant angle σ oscillates around a value close to σ_0. The amplitude of these oscillations, however, grows, indicating the instability of the libration point. Indeed, we performed the numerical linearization of Eqs. (18) around the libration point for $\beta = 0.01$ and we solved the cubic equation for the eigenvalues of the corresponding matrix, obtaining one real negative root and two complex conjugate roots with a positive real part. The small oscillations around the libration point must grow exponentially with time and no permanent capture very close to the libration point may be expected.

Substantial contribution to the problem of resonance trapping was made recently by Weidenschilling & Jackson (1993), who obtained some criteria for trapping of grains in exterior resonances and maximum eccentricities $e_{\max}$ which the eccentricity of captured particles approaches ($e_{\max}$ depends on the resonance). Their value of $e_{\max}$ is always higher than our e_0 but the difference is small ranging from 0.010 to 0.014. Weidenschilling & Jackson's (1993) approach consists in truncation of the resonant part of the perturbing function to the first degree in eccentricity and averaging is made by omitting the non-resonant terms. Their approach is, therefore, valid only for small eccentricities. Very nice formula for increase of captured particle eccentricity (which approaches $e_{\max}$ exponentially) is given. However, for e close to $e_{\max}$ the disturbing function as series in e diverges (see Fig. 12) and the applicability of truncated disturbing function is questionable. It was for instance shown that for higher eccentricities this approach is unable to reproduce families I_e and II_e of periodic orbits in the three body problem (Hadjidemetriou 1993). We made numerical averaging of disturbing function so that our results are not restricted to small eccentricities. Neither our e_0 nor their $e_{\max}$ depend on disturbing function or its coefficients. That is why the differences between them are not very large even if the series for the disturbing function diverges. Our Eq. (19) was obtained and solved for e_0 without any restrictions to lower powers of eccentricity. That is why e_{max} must be considered as approximation of more exact value e_0.

6. Discussion and conclusions

We have studied a simplified planar circular problem of a dust particle motion in the gravitational field of the Sun and one planet (the Earth). The radiation forces were included. We found two libration points for each of the resonances 4/5, 5/6 and 7/8 and for each β (Figs. 14–16). As the PR drag leads to a decreasing semimajor axis a and eccentricity e, we assumed

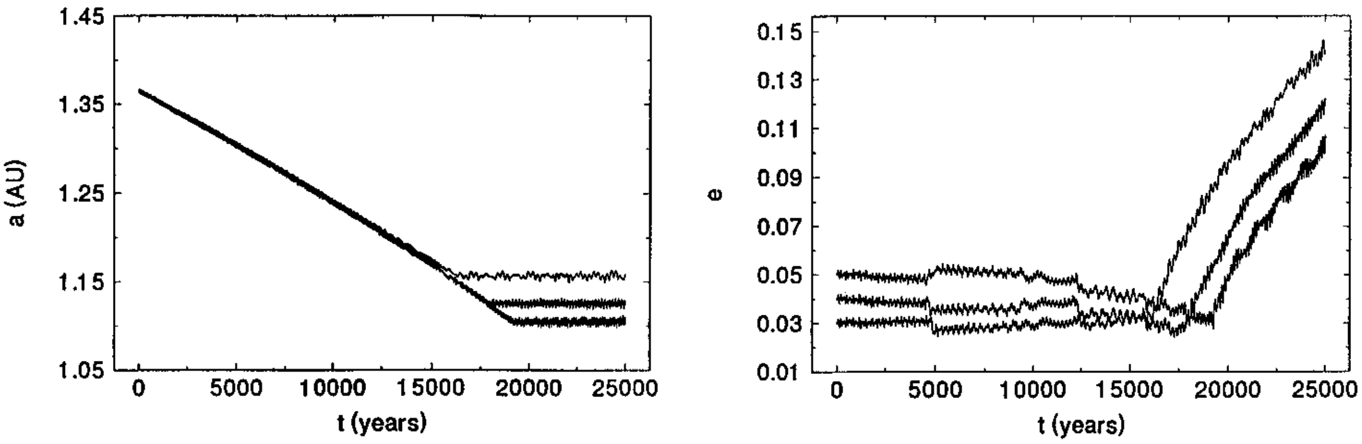

Fig. 17. Three particles are captured in the $4/5$, $5/6$ and $6/7$ resonances with Earth in the general model

for simplicity that the orbit was circularized before the particle approaches resonant a. Numerical simulation showed that if the particle is placed close to the outer edge of the resonance in a circular orbit, it can be temporarily captured when crossing the resonant a. The capture probability depends on β and on the resonance. For $\beta = 0.01$ there is distinct difference between the 4/5 and 5/6 resonance as all 36 test particles crossed the former and all 36 particles were captured in the latter resonance. This well-defined boundary shifts to lower degree resonances with decreasing β, and vice versa.

In practice the eccentricity of the particle (even if initially $e = 0$) will increase slightly (to values e smaller than 0.05) when crossing the outer resonances 1/2, 2/3, 3/4. This nonvanishing eccentricity will change the pattern and some particles may be captured even in the 4/5 resonance (for $\beta = 0.01$), some in the 5/6, etc. (see Sect. 2).

Our previous investigations were based on the simple planar and circular model. We included all planets in our numerical integration in order to show that resonance trapping is a real phenomenon in the solar system. Since we are mainly concerned in near-Earth resonances we chose particles with initial semimajor axis $a = 1.37$ AU. The set of more than one hundred particles $\beta = 0.01$ with $0 \leq e \leq 0.15$ and inclinations $i \leq 10^o$ were released in various angular positions along the initial ellipse.

Figure 17 shows the capture of three particles in different resonances. The particle released with $e = 0.03$ was captured at ~ 1.156 AU into $4/5$, the particle relased with $e = 0.04$ was captured into the middle $5/6$ resonance, and the one with $e = 0.05$ was captured at ~ 1.104 AU in $6/7$. One can see on eccentricity evolution jumps due to 2/3 and 3/4 passing and the typical boost in the capture. The behaviour is qualitatively similar to that observed in the simple model and predicted by analytical treatment.

But capture times are much shorter. They are usually of the order of 1000 y although several captures with times $> 15\,000$ y occurred. And several other things are worth mentioning. The integration confirmed the inefficiency of low-order resonances. We did not observe the 2/3 capture, and the 3/4 capture was rare. The particles with $e > 0.08$ are not usually captured or they are captured for a very short time, then released and finally transferred inside the Earth's orbit. On the other hand, almost every particle with lower eccentricity was captured and spent several thousand years in resonance. The last thing to be mentioned here is that the initial angular positions were found to be unimportant for the particles fate, i. e. particles in different positions on the initial ellipse behave similarly, all of them are either trapped into some resonance or passed through. The full problem with all planets was thus found more complicated (the effect of temporary capture is still there) and the circular problem is just first step to its understanding.

If there is significant component of low eccentricity particles at low inclinations the effect of temporary capture (of order $10^4 - 10^5$ years for the circular and 10^3 years for full problem) might lead to the density distribution peak in the region $1.06 < a < 1.15$. Interplanetary dust can originate in comets, collisions in the asteroid belt, or interstellar clouds or can be remnants of the early solar nebula (Weinberg & Sparrow 1992). As cometary particles come to the Earth's vicinity usually with quite high eccentricity (Jackson & Zook 1992) the temporarily captured particles come most probably from collisions in asteroid belt. The Infrared Astronomical Satellite (IRAS) discovered at least three parallel bands of dust roughly straddling the plane of ecliptic, see more detailed discussion by Sykes et al. (1989). The central bend was later separated into two pairs of bands α and β still between $\pm 3.5°$ of ecliptic latitude. Two theories of origin of the dust bands were suggested. The collisional equilibrium theory assumes that the dust population at a given location is related to the population of observable asteroids at the same location. For nonequilibrium (random collision) hypothesis dust bands are products of stochastic process in which they are created and destroyed over geologic time. Both theories can explain α and β bends and their relationships to Themis and Koronis families (Sykes at al. 1989). Due to PR drag the orbits of particles in α and β bands have to decay. To obtain a rough estimate of their eccentricity when the Earth orbit is passed we use an integral found by Wyatt & Whipple

$$K = a(1 - e^2)e^{-\frac{4}{5}}. \tag{22}$$

Using e and a for Themis and Kronis we get K = 15.17 AU (Themis) and K = 30.67 AU (Koronis). When the semimajor axis of the particle approaches a = 1 AU we can approximate corresponding eccentricity

$$e = K^{-\frac{5}{4}}, \tag{23}$$

yielding $e \sim 0.03$ for Themis and $e \sim 0.013$ for Koronis. This example shows that the α and β bands which are permanent features in the collisional equilibrium theory could supply the low eccentricity and low inclination particles as eccentricity is reduced during the orbital evolution.

Example of Themis shows that the eccentricity of the parent body may be as large as 0.13 and the eccentricity of particle in the Earth's vicinity is reduced to 0.03. These arguments widen the set of asteroid eligible as sources for low eccentricity particles which may be temporarily captured at the Earth's exterior resonances (and contribute to formation of peak) as described above.

Due to the β-dependence of resonant a one cannot expect individual sharp peaks for the individual resonances. On the other hand, e is independent of β and clear individual peaks at values given by Table 1 in the eccentricity distribution should be formed. This approach gives at least a qualitative prediction of the fine structure of the grain distribution in the vicinity of the Earth's orbit. For any quantitative prediction we need to know the distribution (in eccentricity, inclination, β) of grains incoming from outer space to the Earth's vicinity.

Acknowledgements. We thank an anonymous referee for his constructive criticism.

References

Beaugé C., 1993, Celest. Mech. & Dynam. Astron. in press
Beaugé C., Ferraz-Mello S., 1993a, Icarus 103, 301
Beaugé C., Ferraz-Mello S.,1993b, Icarus in press
Burns J. A., Lamy P. L., Soter S., 1979, Icarus 40,1
Ferraz-Mello S., 1993, submitted to Celest. Mech. & Dynam. Astron.
Ferraz-Mello S., Tsuchida M., Klafke J. C., 1993, Celest. Mech. & Dynam. Astron. 55, 25
Gonzi R., Froeschle Ch., Froeschle Cl., 1982, Icarus 51, 633
Hadjidemetriou J. D.. 1993, Celest. Mech. & Dynam. Astron. 56, 201
Jackson A. A., Zook H. A., 1992, Icarus 97, 70
Message P. J., 1958, AJ 63, 443
Quinlan G. D., Tremaine S., 1990, AJ 100, 1694
Sicardy B., Beaugé C., Ferraz-Mello S., Lazzaro D., Roques F., 1994, Celest. Mech. 57, In press
Šidlichovský M., 1991, Bull. Astron. Inst. Czechosl. 42, 116
Sundman K., 1916, Öfversigt at Finska Vetenskaps-Societetens Förhandlingar. 58A(24), 1
Sykes M. V., Greenberg R., Dermott S. F., Nicholson P. D., Burns J. A., 1989, Dust Bands in the Asteroid Belt, in Asteroids II, (eds. R. P. Binzel, T. Gehrels, M. S. Matthews) p. 336, the Univ. of Arizona Press
Weidenschilling S. J., Davis D. R., 1985, Icarus 62, 16
Weidenschilling S. J., Jackson A. A., 1993, Icarus 104, 244
Weinberg J. L., Sparrow J. G., 1992 in Cosmic Dust, ed. J. A. M. McDonnell, p. 75, John Willey &Sons, Chichester–New York–Brisbane–Toronto
Wyat S. P., Whipple F. L., 1950, ApJ 111, 134

This article was processed by the author using Springer-Verlag LaTeX A&A style file version 3.